Author Manuscript

Author Manuscript

Author Manuscript

Author Manuscript

HHS Public Access

Author manuscript

J Immunol. Author manuscript; available in PMC 2019 May 15.

Published in final edited form as:

J Immunol. 2018 May 15; 200(10): 3612–3625. doi:10.4049/jimmunol.1701287.

Inflammatory macrophage expansion in pulmonary hypertension depends upon mobilization of blood-borne monocytes

Jonathan Florentin[1], **Emilie Coppin**[1], **Sathish Babu Vasamsetti**[1], **Jingsi Zhao**[1], **Yi-Yin Tai**[1], **Ying Tang**[1], **Yingze Zhang**[2], **Annie Watson**[1], **John Sembrat**[1,3], **Mauricio Rojas**[1,3], **Sara O. Vargas**[4], **Stephen Y. Chan**[1,*], and **Partha Dutta**[1,5,*]

[1]Center for Pulmonary Vascular Biology and Medicine, Pittsburgh Heart, Lung, Blood, and Vascular Medicine Institute, Division of Cardiology, Department of Medicine, University of Pittsburgh School of Medicine and University of Pittsburgh Medical Center, BST 1720.1, 200 Lothrop Street, Pittsburgh, PA 15213, USA

[2]Department of Medicine, University of Pittsburgh, Pittsburgh, PA, USA

[3]Division of Pulmonary, Allergy and Critical Care Medicine, University of Pittsburgh, PA, 15261, USA

[4]Department of Pathology, Boston Children's Hospital, Boston, MA, 02115, USA

[5]Department of Immunology, University of Pittsburgh School of Medicine, PA 15213, USA

Abstract

Pulmonary inflammation, characterized by the presence of perivascular macrophages, has been proposed as a key pathogenic driver of pulmonary hypertension (PH), a vascular disease with increasing global significance. However, the mechanisms of expansion of lung macrophages and the role of blood-borne monocytes in PH are poorly understood. Using multicolor flow cytometric analysis of blood in mouse and rat models of PH and patients with PH, an increase in blood monocytes was observed. In correlation, lung tissue displayed increased chemokine transcript expression, including those responsible for monocyte recruitment such as *Ccl2* and *Cx_3cl1,* accompanied by an expansion of interstitial lung macrophages. These data indicate that blood monocytes are recruited to lung perivascular spaces and differentiate into inflammatory macrophages. Correspondingly, parabiosis between congenically different hypoxic mice demonstrated that most interstitial macrophages originated from blood monocytes. To define the actions of these cells in PH *in vivo*, we reduced blood monocyte numbers via genetic deficiency of *cx_3cr1* or *ccr2* in chronically hypoxic male mice and by pharmacologic inhibition of Cx_3cl1 in monocrotaline-exposed rats. Both models exhibited decreased inflammatory blood monocytes as well as interstitial macrophages, leading to a substantial decrease of arteriolar remodeling but with a less robust hemodynamic effect. This study defines a direct mechanism by which interstitial

Corresponding Authors: Partha Dutta, PhD, Assistant Professor of Medicine and Immunology, Vascular Medicine Institute, Division of Cardiology, Department of Medicine, University of Pittsburgh Medical Center, BST 1720.1, 200 Lothrop Street, Pittsburgh, PA 15213, USA, Tel: 412-383-7277, duttapa@pitt.edu. Stephen Y. Chan, MD, PhD, Center for Pulmonary Vascular Biology and Medicine, Pittsburgh Heart, Lung, Blood, and Vascular Medicine Institute, Division of Cardiology, Department of Medicine, University of Pittsburgh School of Medicine, University of Pittsburgh Medical Center, 200 Lothrop Street BST1704.2, Pittsburgh, PA USA 15261, Tel: 412-383-6990, Fax: 412-624-9160, chansy@pitt.edu.

*These authors contributed equally to this work

Author Manuscript Author Manuscript Author Manuscript Author Manuscript

macrophages expand in PH. It also demonstrates a pathway for pulmonary vascular remodeling in PH that depends upon interstitial macrophage-dependent inflammation yet at least is partially dissociated from hemodynamic consequences, thus offering guidance on future anti-inflammatory therapeutic strategies in this disease.

Introduction

Pulmonary hypertension (PH) is a progressive cardiopulmonary disease characterized by elevated mean pulmonary arterial pressure at rest, leading to right ventricular failure, multi-organ dysfunction and often death. While heterogenous in nature, the most severe cases of PH, including pulmonary arterial hypertension (PAH), are characterized by histologic alterations including medial hypertrophy, intimal and adventitial thickening, and the formation of occlusive plexiform lesions in small to medium-sized pulmonary arteries. However, it is not known whether both the histologic and hemodynamic manifestations of this disease are similarly regulated at the molecular level or whether each manifestation contributes independently to disease progression and patient survival. The vascular manifestations of PH are associated with cellular and soluble inflammatory mediators [1–3]. There is growing appreciation that pulmonary vascular inflammation, involving multiple hematologic and tissue-resident immune cells, plays a key role in the development and progression of PH [4–6]. Such pathobiology has supported the notion of developing novel anti-inflammatory therapies in PH [7], since currently approved PH therapies do not cure, prevent, or regress this disease. Notably, anti-inflammatory therapies may act as anti-remodeling agents, thus differing from available pulmonary vasodilators, which primarily control vasomotor tone and dilate partially occluded pulmonary arteries [8, 9]. It remains unclear whether hemodynamic improvement adequately reflects vascular remodeling *in vivo* and whether hemodynamics should be used as the primary index of efficacy of emerging anti-inflammatory drugs in this disease.

Myeloid leukocytes, especially macrophages [10, 11], are among the primary effectors of inflammation in pulmonary lesions in PH patients. A role of macrophages in aggravating PH pathogenesis has been proposed [11–13]. While alveolar macrophages participate in local immune homeostasis and have certain surfactant properties [14, 15], lung interstitial macrophages, such as perivascular macrophages, play a major role in lung inflammation [16] and function [16–20] in diseases like PH. However, the origin of lung perivascular macrophages in PH has not been fully described. Recently, it was reported that activation and expansion of lung alveolar and interstitial macrophages is time- and anatomic space-dependent [21]. Prior work suggested that expansion of lung macrophages in PH is dependent on circulating blood-borne progenitors [2]. Moreover, a recent study demonstrated that TGF-β activation in the lungs by hematopoietic cell-derived thrombospondin-1 could trigger *Schistosoma mansoni*-induced PH [22]. However, the precise dynamics, origin, and pathobiological roles of different lung macrophage subsets in PH have not been described, and, in particular, the exact identity of the blood-borne cells contributing to the lineage of lung macrophages in PH has not been defined.

Author Manuscript Author Manuscript Author Manuscript Author Manuscript

Circulating monocytes represent a possible upstream progenitor of lung interstitial macrophages in PH, given their importance in contributing to the interstitial macrophage population at steady state [23]. Prior lineage tracing experiments have indicated that tissue resident macrophages including alveolar lung macrophages are derived independently either from yolk sac or fetal liver progenitors before birth [24]. In general, hematopoietic cells, including macrophages, are produced by 'primitive' and 'definitive' hematopoiesis [25]. During primitive hematopoiesis in the embryonic stage, yolk sac-derived progenitors give rise to primitive myeloid cells including monocytes [26], and later, tissue macrophages that can self-maintain in tissues by local proliferation [26]. Monocytes are innate immune cells that specialize in phagocytosis, antigen presentation, and inflammation. In mice, monocytes fall into two main subsets: proinflammatory Ly-6c^{high} Cx$_3$cr1^{low} [27] and patrolling Ly-6c^{low} Cx$_3$cr1^{high} [28]. Humans have three distinct monocyte subsets: CD14^{high} CD16^{low} (inflammatory, classical), CD14^{high} CD16^{int} (intermediate), and CD14^{int} CD16^{high} (patrolling, non-classical) [29]. In some inflammatory diseases, non-classical monocytes have been shown to have pro-inflammatory features [30–32]. Chemokine receptors such as CX$_3$CR1 and CCR2 help the egress of monocytes from the bone marrow [17, 28, 33–35]. Once in the blood circulation, monocytes travel along a chemokine gradient and infiltrate into sites of injury. Deficiency in CCR2 expression results in decreased numbers of recruited monocytes at sites of inflammation [36].

In the present study, we aimed to determine the contribution of circulating monocytes in the expansion of perivascular macrophages, particularly interstitial macrophages, in PH and to define the role of circulating monocytes in PH pathogenesis. To do so, we employed multicolor flow cytometric analysis coupled with the availability of both blood and lung tissues from multiple animal models and human patients of PH. Consequently, we delineated a direct mechanism by which interstitial macrophage expansion occurs in PH. By both genetic and pharmacologic depletion of blood monocytes in rodent models of disease, we demonstrated that interstitial macrophages are derived from blood-borne monocytes and play a robust role in pulmonary vascular remodeling in PH but have a less prominent effect on hemodynamics. Thus, these results define the cellular origin of inflammatory macrophages in PH. They also demonstrate specific patho-phenotypic actions of these cells *in vivo*, and begin to delineate an inflammatory-mediated distinction between histologic and hemodynamic aspects of this disease.

Materials and Methods

Human samples and cell storage

PAH patient lung samples (n=6) or control lung samples (n=5) were collected from the University of Pittsburgh Medical Center and Boston Children's Hospital. Lungs and peripheral blood from PAH patients and healthy donors were collected and processed as described below. A piece of lung was weighed and minced into small pieces and digested in enzymatic mixture containing 450 U/mL collagenase I, 125 U/mL collagenase XI, 60 U/mL DNase I, and 60 U/mL hyaluronidase (Sigma-Aldrich) at 37°C at 750 rpm for 1 h. Cells were passed through 40-μm cell strainer, washed in 10 ml FACS buffer and centrifuged (4°C, 370 g, 7 minutes). Two to three mL of concentrated EDTA-treated blood were

Author Manuscript Author Manuscript Author Manuscript Author Manuscript

collected and diluted twice. Leukocytes were separated from total blood by a Ficoll gradient. Briefly, the whole diluted blood was carefully added on top of the Ficoll. The cells were then centrifuged at 350g for 40 minutes at 4°C. The leukocyte ring was then collected and washed into 10 mL of fresh DMEM, centrifuged at 350 g for 10 minutes at 4°C. Lung and blood cells were then counted using Trypan Blue (Cellgro, Mediatech, Inc, VA) and resuspended at 1 million/mL in freezing medium (70% DMEM, 20% FBS and 10% DMSO v/v) and then aliquoted in cryovials and stored in liquid nitrogen.

Animals

All animal experiments were conducted following NIH guidelines under protocols approved by the Institutional Animal care and Use Committee of the University of Pittsburgh. We chose to study the chronically hypoxic mouse as a first-line model of PH, because of its long-standing use in PH research and because of the well-established genetic tools and flow cytometric protocols in studying myeloid populations. Adult male C57BL/6 wild type, *cx$_3$cr1* GFP/GFP, *ccr2* KO and *ubiquitin*-GFP mice (10–12 weeks old) were obtained from Jackson Lab and maintained under a standard light cycle (12h light/dark). To induce pulmonary hypertension, mice were put for 3 weeks in hypoxic chamber under normobaric 10% O_2. To track the cellular origin of interstitial macrophages, adult C57BL/6 wild type and *ubiquitin*-GFP male mice were surgically joined from the hip to the shoulder for 3 weeks. The blood chimera level was tested prior putting the parabiosed mice in hypoxic chamber for another 3 weeks. Adult male Sprague-Dawley rats (8–12 weeks old) were obtained from Charles River. To induce pulmonary hypertension, rats were injected once with 60 mg/kg of monocrotaline. Such monocrotaline-exposed rats tend to display pronounced pro-inflammatory features and have served for years as a long-standing and well-established model of experimental PH. Thus, this model served as an appropriate complement to the hypoxic mouse, since any molecular similarities found in both models would likely be broadly relevant across different subtypes of PH. To study the impact of monocyte recruitment into the lungs in the context of pulmonary hypertension, rats were also injected daily with 10 μg of Cx_3cl1 inhibitor for 3 weeks (RnD Systems).

Organ harvesting and flow cytometry

Mice were euthanized and perfused thoroughly with 30 ml of ice cold PBS through the left ventricle. The upper lobe of the right lungs was harvested, minced into small pieces and digested in enzymatic mixture containing 450 U/ml collagenase I, 125 U/ml collagenase XI, 60 U/ml DNase I, and 60 U/ml hyaluronidase (Sigma-Aldrich) at 37°C at 750 rpm for 1 h. Cells were passed through 40-μm cell strainer, washed in 10 ml FACS buffer and centrifuged (4°C, 370 g, 7 minutes). Peripheral blood was collected through retro-orbital bleeding. Erythrocytes were lysed using ACK lysis buffer for 3 minutes and 3 ml of FACS buffer was added and centrifuged. Supernatant was carefully discarded and pellet was dissolved in FACS buffer (PBS containing 0.5% bovine serum albumin). Leukocytes were washed and resuspended in FACS buffer. Total viable cell numbers were obtained from above aliquots using Trypan Blue (Cellgro, Mediatech, Inc, VA). Following harvesting of single cell suspensions, cells were stained in FACS buffer. All antibodies used in this study were purchased from eBioscience, BioLegend or BD Biosciences. For myeloid cells panel analysis, monoclonal antibodies including anti-CD11b (M1/70), CD19 (6D5), CD115

Author Manuscript Author Manuscript Author Manuscript Author Manuscript

(AFS98), Ly6G (1A8), Ly6C (HK1.4), CD103 (M290) and CD64 (X54–5/7.1.1) were used. Ly-6c^{low} monocytes were identified as CD11b^{+} CD115^{+} Ly-6c^{low} and Ly-6c^{high} monocytes were defined as CD11b^{+} CD115^{+} Ly6c^{high}. Alveolar macrophages were identified according to Misharin et al., 2013 [23] as CD11b^{+}, CD19^{+}, CD64^{+} and CD103^{+}. Interstitial macrophages were identified according to Misharin et al., 2013 [23] as CD11b^{+}, CD19$^{−}$, CD64^{+} and CD103^{+}. Human cells were stained using the same protocol as mouse cell staining. For myeloid cell panel analysis, monoclonal antibodies including anti-CD45 (HI30), CD14 (61D3), CD16 (3G8), CD24 (ML5), HLA-DR (G46–6), CD169 (7–239) and CD206 (19.2) were used. Classical monocytes were identified as CD14^{high} and CD16^{low}. Intermediate monocytes were identified as CD14^{high} and CD16^{int}. Non-classical monocytes were identified as CD14^{int} and CD16^{high}. Alveolar macrophages were identified as CD206^{+}, CD14^{+} and CD169^{+}. Interstitial macrophages were identified as CD206^{+}, CD14^{+} and CD169$^{−}$. Cell numbers per mg of tissue for lungs, and mL of blood were calculated as total cells per lung and mL of blood sample multiplied by percentage of cells obtained from the appropriate FACS gates. Data acquisition was performed using Fortessa Flow Cytometer (BD). Data were analyzed using with FlowJo software (Tree Star).

Immunofluorescence

Following perfusion, lungs were removed, fixed in 4% PFA (paraformaldehyde, methanol-free, Electron Microscopy Science) for 1 h and immersed in PBS containing 30 % sucrose and 0.05 % sodium azide overnight at 4°C. Then tissue was embedded in Tissue-Tek® OCT compound (Sakura Finetek), and frozen on dry ice. For immunofluorescence staining, sections of 20 μm were rehydrated with PBS and permeabilized with 0.1% (v/v) Triton X-100 for 1 h at room temperature. Following blockade with blocking solution (PBS+ 2% BSA) for 1 h, sections were incubated with anti-CD68 (clone EPR1344, Abcam), anti-SMA-Cy3 (Millipore) for 1 h. The sections were subsequently washed with PBS + 0.5% BSA and incubated with anti-mouse secondary antibody conjugated with FITC. The sections were counterstained and fixed with vector shield DAPI to visualize nucleus and images were taken using Confocal laser scanning immunofluorescence microscopy (CLSM). Image analysis was done using Image J software (Fiji). Human lungs from control donors or from PH patients were processed the same way as mouse lungs. Following blockade, sections were incubated with anti-CD68 (clone EPR1344, Abcam), anti-SMA-Cy3 (Millipore) and anti-CD14 for 1 h. Rat lung sections were stained with anti-CD68 (clone ED1, Bio-Rad), anti SMA-Cy5 (Millipore), anti-CD31 (clone H3, Santa Cruz) for 1 h. Small pulmonary vessels (10 vessels per section) that were not associated with bronchial airways were selected for analysis (N>5 animals per group). Intensity of staining was quantified using ImageJ software (Fiji). Degree of pulmonary arteriolar muscularization was assessed in paraffin-embedded lung sections stained for α-SMA by 17 calculation of the proportion of fully and partially muscularized peripheral (<100 mm diameter) pulmonary arterioles to total peripheral pulmonary arterioles, as previously described (29). Medial thickness was also measured in α-SMA stained vessels (<100 mm diameter) using ImageJ software (Fiji) and expressed as arbitrary units. All measurements were performed blinded to condition.

Author Manuscript Author Manuscript Author Manuscript Author Manuscript

qRT-PCR

Following collection, lungs were cut into small pieces and flash frozen in liquid nitrogen. Total mRNA was extracted using RNeasy RNA isolation kit (Qiagen) and cDNA was prepared from 100 ng of mRNA with the high capacity RNA to cDNA synthesis kit (Applied Biosystems). Quantitative RT-PCR was performed using SYBR green primers (IDT) and results were expressed as Ct values normalized to the house-keeping gene *beta-actin* (with the control set as 1).

Right heart catheterization and tissue harvest

On day 21 of hypoxia, right ventricular catheterization was performed followed by tissue and blood collection. The mice were anesthetized with ketamine/xylazine and ventilated through a trans-tracheal catheter. The abdominal and thoracic cavities were opened, and a 1Fr pressure-volume catheter (Millar PVR-1035, Millar Instruments) was placed through the right ventricle apex to transduce the pressure. Heart was flushed with 10 mL of PBS and removed, followed by dissection and weighing of the right ventricle (RV) and of the left ventricle + septum (LV+S). Organs were then harvested for histological preparation, flowcytometric experiments, or flash frozen in liquid N2 for subsequent homogenization and extraction of RNA and/or protein.

Statistical analysis

Data are represented as mean±SEM. Statistical significance between groups was performed using two-tailed Student *t* test or ANOVA according to the data set. Results were considered as statistically significant when $P<0.05$.

Study approval

All animal experiments were approved by the University of Pittsburgh Institutional Animal Care and Use Committee. All experimental procedures involving the use of human lung tissue included the relevant receipt of written informed consent and were approved by the Committee for Oversight of Research and Clinical Training Involving Decedents No. 101, at the University of Pittsburgh, as well as the Institutional Review Board of the University of Pittsburgh No. REN17020169/IRB020810 and the Institutional Review Board at Boston Children's Hospital. All experimental procedures involving the use of human peripheral blood included the relevant receipt of written informed consent and were approved the Institutional Review Board of the University of Pittsburgh No. REN16070123/PRO11070366 as well as the Institutional Review Board of the University of Pittsburgh No. REN17030011/IRB0306040. Ethical approval for this study and informed consent conformed to the standards of the Declaration of Helsinki.

Results

Interstitial macrophage and monocyte populations expand in the lungs of hypoxic mice, monocrotaline-injected rats, and PH patients

To quantify the alterations of specific subsets of lung and pulmonary vascular macrophages in PH, we studied multiple animal and human models of PH, including mice with hypoxia-

Author Manuscript Author Manuscript Author Manuscript Author Manuscript

induced PH, rats with monocrotaline-induced PH and human PH patients. In the lungs of hypoxic mice with PH as compared to normoxic mice (hemodynamics and remodeling score shown in Figure S1A and B respectively), we enumerated alveolar and interstitial macrophages by multicolor flow cytometry (Figure S1C) at different time points of hypoxia exposure. In hypoxic mice, we found a gradual loss of alveolar macrophages and significantly increased number of interstitial macrophages (Figure 1A–B). Next, we investigated the mechanisms of the disappearance of alveolar macrophages. Flow cytometry analysis of the cell cycle status of alveolar macrophages did not reveal any change in proliferation (Figure S1D). We observed increased expression of cleaved caspase 3 in alveolar macrophages of hypoxic mice, indicating augmented apoptosis of these macrophages under hypoxic condition (Figure 1C and S1E). To determine the mechanisms of increased apoptosis of alveolar macrophages in hypoxic mice, we assessed the levels of granulocyte-macrophage colony stimulating factor (*gm-csf*), important for alveolar macrophage maintenance [37] and *m-csf*, necessary for tissue resident macrophage survival in the lungs [38]. The level of *gm-csf* was significantly decreased in hypoxic mice. However, *m-csf* expression was not altered in hypoxic mice compared to normoxic control (Figure 1D).

In parallel, perivascular lung macrophages were observed in monocrotaline-exposed PH rats (hemodynamics shown in Figure S1F), a well-established model of PAH with significantly increased inflammation in the lungs [39]. Because of the lack of well-characterized anti-rat antibodies for flow cytometry, confocal imaging of lung sections of monocrotaline versus PBS-injected rats was performed, and the expansion of $CD68^+$ macrophages specifically in the pulmonary arteriolar compartment was confirmed (Figure 1E–F). Finally, we quantified lung macrophages from human PH patients (clinical demographics and hemodynamics catalogued in Table S1A). Notably, alterations in lung macrophage subsets of PH patients were similar to those seen in hypoxic mice (Figure 1G & 1H and Figure S1G).

Given the direct differentiation of macrophages from inflammatory monocytes in other contexts of inflammation [40], we also enumerated monocytes in the lungs of hypoxic mice (Figure S2A). We confirmed that the number and percentage of monocytes were gradually increased in the lungs of mice after hypoxia exposure at different time points of hypoxia (Figure 2A–B). Similarly, we observed a significant increase in number and percentage of non-classical lung monocytes in PH patients (Figure 2C–D, Figure S2B). Confocal imaging confirmed the accumulation of $CD14^+$ $CD68^-$ monocytes as well as $CD14^+$ $CD68^+$ interstitial macrophages in the arteriolar compartment and interstitium in the patients (control, 1±0.48 vs. PH, 3.8±0.64) (Figure 2E–F). Taken together, these data demonstrate a parallel expansion of both monocytes and perivascular interstitial macrophages across multiple instances of PH lung tissue in rodents and humans. Additionally, we found decreased alveolar macrophage numbers in the lung of hypoxic mice and PH patients.

Inflammatory monocytes are increased in the blood of hypoxic PH mice and human PAH patients

Given the increase of macrophages and monocytes across diseased PH lungs, we also assessed blood-borne monocyte populations in both hypoxic PH mice and human PH

Author Manuscript Author Manuscript Author Manuscript Author Manuscript

patients. In hypoxic mice, both the percentage (Figure 3A) and the number (Figure 3B) of circulatory monocytes, including pro-inflammatory Ly-6c^{high} monocytes, increased at different time points after hypoxic exposure [41]. We also quantified blood monocyte populations in human PH patients (demographics and hemodynamics catalogued in Table S1A and S1B). Consistent with the monocytosis in hypoxic mice, we found that these patients displayed higher number of circulating monocyte subsets (control, $3.9.10^4 \pm 2.3.10^4$ vs. PH, $3.2.10^5 \pm 1.2.10^5$) (Figure 3C–D). We wanted to assess the possible discrepancies in monocyte number and frequency between PAH scleroderma and PAH idiopathic patients. No significant difference in monocyte number and frequency was observed (Figure S2C).

Notably, due to the scarcity of available human lung tissue and blood from human PH patients and the logistical difficulties in precisely timing appropriate sample procurement, it has been exceedingly challenging to analyze matched blood and lung tissue from the same PH patient, thus indicating only an indirect association of blood monocytosis and lung macrophage expansion in humans. Stemming from the tremendous generosity of a single PH patient who donated both blood and lung tissue immediately after death, we enumerated both monocyte and interstitial macrophage populations in both blood and lungs. Consistent with our findings in rodents and humans, increased frequency of non-classical monocytes in the blood and lungs (Figure 3E) correlated with increased monocytes and interstitial macrophages in pulmonary vascular compartment (Figure 3F). Thus, in aggregate, both hypoxic PH mice and PH patients display an inflammatory monocytosis in both blood and lung tissue, which correlates with increased interstitial macrophages in the lungs and pulmonary vascular compartment.

Monocyte and macrophage expansion in PH lungs promotes a pro-inflammatory milieu

To determine the extent of an inflammatory environment promoted by monocyte and macrophage expansion, we quantified chemokine and cytokine production in the lungs of PH patients based on known inflammatory signaling in other contexts (summarized in Figure 4A). The lungs of hypoxic mice displayed increased levels of chemokines and pro-inflammatory cytokines such as *cx$_3$cl1, ccl2, il1b, il6, il18* and *tnfa* (Figure 4B) [28, 41]. Lungs of PH patients demonstrated similar pattern of inflammatory gene expression (Figure 4C). Additionally, we found an increased level of chemokines in the lungs of PH patients, such as *CCL1*, *CCL2*, *CCL3*, *CCL4* and *CX$_3$CL1* (Figure 4C and Figure S2D), factors known to induce migration of monocytes [42]. To assess the change of phenotype of circulating monocytes in PH, we sorted these cells from the blood of PH patients using fluorescence activated cell sorting. Importantly, circulatory monocytes in PH patients displayed augmented expression of corresponding chemokine receptors such as *CCR1*, *CCR2*, *CCR5* and *CX$_3$CR1* (Figure 4D & S2E). Interestingly, phenotype of blood monocytes isolated from PH patients mirrored the lung inflammatory micro-environment (Figure 4D). To ascertain the progressive change of phenotype of blood monocytes after hypoxia exposure, we sorted these cells from the blood of hypoxic mice. Monocytes sorted at day 3 and 12 of hypoxia displayed gradual increase in the expression of the chemokine receptors *ccr2* and *cx3cr1* (Figure S2F). Concomitantly, the levels of the pro-inflammatory cytokines *il1b*, *il6* and *tnfa* progressively increased in sorted monocytes. These data indicate their active recruitment into the lungs as well as their conversion from non-inflammatory to

Author Manuscript Author Manuscript Author Manuscript Author Manuscript

pro-inflammatory phenotype. Next we investigated the mechanisms of egress of bone marrow monocytes immediately after hypoxia exposure. Since bone marrow niche cells such as endothelial cells (EC), mesenchymal stem cells (MSC) and osteoblasts (OST) secrete factors, such as *ccl1*, *ccl2* and *cx$_3$cl1*, which retain monocytes in the bone marrow at steady state[43], we sorted these niche cells and quantified these retention factors using qPCR. Our analysis demonstrated significant decreases of these retentions factors in the niche cells sorted from hypoxic mice compared to normoxic controls (Figure S2G). Collectively, these data demonstrate a proinflammatory monocyte and macrophage milieu in PH reflected in both blood and lung tissue. More specifically, elevation of chemokines in the lungs and increased chemokine receptor expression in blood monocytes indicate there are specific signals for mobilization of monocytes from the blood to the lungs.

Interstitial macrophages but not alveolar macrophages are derived from infiltrating blood monocytes in the lungs of hypoxic mice

To test directly the hypothesis that inflammatory blood monocytes are the source of pulmonary perivascular interstitial macrophages in PH, we studied a model of parabiosis whereby the circulatory systems of two congenically distinct mice were joined surgically. Three weeks after surgical parabiosis, when the chimera levels reached approximately 30% (Figure 5A and Figure S3A), we placed the parabionts in hypoxic chambers for 3 weeks and quantified the chimera levels in monocytes, and alveolar and interstitial macrophages in the lungs (Figure 5B). Hemodynamic and histologic manifestations of hypoxia-induced PH were observed in both parabionts (Figure S3B). In that setting, the level of chimera for interstitial macrophages reached approximately 70%, while the level of chimera for alveolar macrophages was only 13% (Figure 5C), consistent with a report describing the embryonic origin of alveolar macrophages [37]. Thus, these data demonstrate more than 2/3 of lung interstitial macrophages are derived from blood monocytes (Figure 5C). Moreover, to explore the origin of interstitial macrophages located at the perivascular spaces, we performed immunofluorescence of the lung sections of hypoxic mice. We observed the presence of parabiont-derived perivascular macrophages in the lungs of hypoxic mice (Figure 5D). As a result, we conclude that, at least in the context of hypoxic PH, interstitial perivascular lung macrophages are derived directly from circulating blood monocytes.

Furthermore, these data indicate that resident interstitial macrophages are replaced by infiltrating monocyte-derived interstitial macrophages. To investigate the fate of resident interstitial macrophages in hypoxia, we needed to distinguish these two subsets of interstitial macrophages. Consistent with published reports[23, 44, 45], our parabiosis experiments revealed that host-derived (resident) interstitial macrophages expressed higher levels of MHC class II compared to parabiont (monocyte)-derived interstitial macrophages (Figure S3C). In fact, about 4% of parabiont-derived interstitial macrophages were MHC-II$^+$, while more than 96% of host-derived interstitial macrophages were MHC-II$^+$ (Figure S3D). Enumeration of these two subsets of interstitial macrophages by flow cytometry at different time points after hypoxia initiation revealed that the numbers of both of the cell populations significantly diminished at day 3 and day 12 of hypoxia. However, only the monocyte-derived interstitial macrophage numbers significantly increased at day 21 compared to normoxic controls (Figure 5E). To check the alteration of resident interstitial macrophage

Author Manuscript Author Manuscript Author Manuscript Author Manuscript

phenotype, we sorted resident interstitial macrophages and observed decreased RNA levels of *ccl2* and *cx3cl1*, chemokines involved in monocyte recruitment, and *il1b, il6 and tnf-a*, which are inflammatory cytokines (Figure S3E).

CX_3CR1 and CCR2 deficiencies in rodents exhibit reduced pulmonary inflammation and diminished remodeling of lung vasculature

Numerous studies have proposed the role of monocytes in various diseases [27, 41]. However, the role of monocytes in the exacerbation of inflammation and tissue remodeling in pulmonary hypertension is not known. Monocytes express high levels of the chemokine receptor Ccr2 [46]. This receptor is essential for the egress of monocytes from the bone marrow and their recruitment at sites of inflammation [33, 43]. Monocytes also express high levels of Cx_3cr1, which is involved in their retention and survival [47, 48].

Thus, *cx3cr1* and *ccr2*-deficient mice as compared with wildtype mice were exposed to chronic hypoxia and utilized to explore the role of monocytes in hypoxic PH. First, we enumerated monocyte subsets and interstitial macrophages in the lungs (Figure 6A and 6B), and monocyte subsets in the blood (Figure 6C) of hypoxic mice. In the blood, both *cx3cr1* and *ccr2*-deficient hypoxic mice displayed decreased number of inflammatory myeloid cells compared to hypoxic wild type mice (Figure 6C). A similar reduction in the number of monocytes and interstitial macrophages was observed in the lungs of both hypoxic *cx3cr1* and *ccr2*-deficient mice compared to wild type mice (Figure 6B). The frequency of cells followed the same pattern across all the conditions in blood (Figure S3F) and lungs (Figure S3G) of hypoxic vs. normoxic mice. The expression of genes encoding inflammatory cytokines and chemokines in *cx3cr1* and *ccr2*-deficient mice significantly diminished compared to hypoxic WT mice (Figure 6D). Via *in situ* staining of vascular smooth muscle, pulmonary vascular remodeling, as quantified by arteriolar wall thickness, in both *cx3cr1* or *ccr2*-deficient mice was significantly decreased compared to wildtype mice under hypoxic condition (Figure 6E). Conversely, *cx3cr1* and *ccr2* deficiency did not significantly alter the hemodynamic manifestation of PH, as reflected by right ventricular systolic pressure (RVSP) (Figure 6F).

Cx_3cl1 inhibition in monocrotaline-injected rats limits the recruitment of lung infiltrating monocytes and diminishes pulmonary artery wall remodeling

To determine whether Cx_3cl1 inhibition displayed similar predilection for modulating vascular remodeling in a separate and more inflammatory model of PH, monocrotaline-exposed rats were treated with daily intraperitoneal injections [49]) of a well-characterized neutralizing antibody for Cx_3cl1 as compared with IgG isotype control [49]. By echocardiography, such treatment did not affect left ventricular function or structure (Figure S3H). However, Cx_3cl1 neutralization significantly reduced monocyte and macrophage expansion in the lungs (Figure 7A). As with genetic deficiency in mice, Cx_3cl1 neutralization reduced pulmonary arteriolar remodeling as assessed *in situ* quantitation of α-SMA (Figure 7B). However, similar to *cx3cr1*-deficient mice, Cx_3cl1 neutralization displayed only subtle trends toward improvement of right ventricular systolic pressure (Figure 7C) and right ventricular remodeling (right ventricle mass/left ventricle+septum mass, RV/LV+S) (Figure 7C). In aggregate, these findings demonstrate that Cx_3cl1 and Ccr2

Author Manuscript Author Manuscript Author Manuscript Author Manuscript

are crucial mediators of recruitment of lung infiltrating monocytes in PH and that lung perivascular macrophages derived from blood monocytes actively participate in pulmonary vascular remodeling across various models of PH. Importantly, in contrast to the more robust effects on pulmonary vascular remodeling, hemodynamic manifestations of PH are more subtly altered by such inflammatory mediators.

Discussion

Collectively, via study of both animal and human examples of PH, our data reveal the mechanisms of interstitial lung macrophage expansion in this complex disease. We have found that elevated levels of chemokines in the lungs and increased chemokine receptor expression in blood monocytes initiate mobilization of inflammatory monocytes to the lungs in PH. These monocytes differentiate into interstitial perivascular macrophages, which secrete pro-inflammatory cytokines and contribute to vascular remodeling (Figure 7D). These newly generated monocyte-derived interstitial macrophages replace resident interstitial macrophages. Importantly, via both genetic and pharmacologic means in multiple rodent models of PH, we report that strategies to inhibit Cx_3cl1/Cx_3cr1 signaling and interstitial macrophage expansion potently reduce pulmonary vascular remodeling and inflammation but with less substantial hemodynamic amelioration. Such distinct macrophage-dependent control of primarily histologic rather than hemodynamic parameters of this disease offers insight into the fundamental biology of these inflammatory cells in the pulmonary vasculature as well as guidance into how to translate anti-macrophage therapies into clinical PH practice.

A seminal finding of our work includes direct lineage tracing of hematopoietic-derived blood-borne monocytes to interstitial lung macrophages in PH. In other inflammatory diseases, it has been reported that monocytes are generated from hematopoietic progenitor cells in the bone marrow [27] and spleen [50]. In PH as well, there has been an increasing focus on the importance of bone marrow cells in pathogenesis [20, 51, 52]. For example, hematopoietic cell-derived thrombospondin-1 was found to activate lung TGF-β as a seminal event driving PH due to *Schistomiasis* infection [22]. Additionally, prior work demonstrated that BMPR2 deficiency can drive macrophage expansion in this disease [1], thus connecting the established genetic connection of BMPR2 haplo-insufficiency to bone marrow-derived cells rather than simply pulmonary vascular cell types or cardiomyocytes. A more recent study reported that reconstitution with *bmpr2*-deficient bone marrow in wildtype mice led to aggravated lung remodeling and inflammation in PH [20] and more directly implicating bone marrow mobilization in this process. In light of our current findings linking those hematopoietic processes to the interstitial macrophage via the blood-borne monocyte, it remains to be seen at what stage of myeloid development BMPR2 signaling exerts its primary influence. Furthermore, given the known temporal dependence of human myeloid development from early in development to adulthood, it is possible that myeloid hematopoiesis may be a key determining event in the variable penetrance and genetic anticipation reported in BMPR2-specific cases of hereditary PAH [53]. Our prior work has also demonstrated that in contexts beyond PH, such as myocardial infarction, monocyte expansion is triggered through extramedullary myelopoiesis and accelerates atherosclerosis [42]. Similarly, it is possible that myeloid mobilization in PH may depend

Author Manuscript Author Manuscript Author Manuscript Author Manuscript

upon other extramedullary sources. Given the known association of PH development with splenectomy [54–56], future work will likely link the specific actions of the spleen in PH pathogenesis, potentially via myeloid development. Finally, the upstream triggers that signal to myeloid cells, especially monocytes, for expansion in PH are not known. Different mechanisms of hematopoietic progenitor differentiation into myeloid cells, such as sympathetic activation [57, 58] and danger associated molecular pattern [59], have been proposed in other disease contexts. These or other processes that control myeloid mobilization could factor substantially in the underlying known genetic or environmental triggers of PH that to date have been poorly characterized at a molecular level.

In addition to defining directly blood monocytes as the source of interstitial macrophages, we also observed an increased mobilization of monocyte subsets in both the blood and lung in PH. Yet, the exact role of each of these monocyte populations in PH has yet to be fully described. Monocyte recruitment plays an important role in various sterile inflammatory conditions such as atherosclerosis [60, 61]. During the progression of this disease, both Ly-6C^{high} and Ly-6C^{low} monocytes are recruited to atherosclerotic plaques. CCR2, CCR5 and CX_3CR1 help in Ly-6C^{high} monocyte recruitment into the lesions [62–64], and this monocyte subset is known to differentiate into inflammatory macrophages [65]. Ly-6C^{low} monocytes have phagocytic and pro-angiogenic functions. While their direct role in disease progression is poorly described [66], their behavior in PH may mimic that described recently in coronary artery disease. Myocardial infarction (MI) triggers an acute inflammatory response, with an early peak of circulating inflammatory classical CD14^{+} CD16^{-} monocytes followed by an increase in circulating non-classical CD14^{int} CD16^{+} monocytes [67]. The same pattern of monocyte response has been observed in a mouse model of MI [68]. This temporal difference in the recruitment of monocyte subsets to the infarcted myocardium allows for the removal of dead cardiac myocytes in the first phase and triggers the resolution of inflammation and tissue healing in the second phase [69]. To define the recruitment pattern and functions of monocyte subsets in PH, future studies will be required for specific depletion of each monocyte subset *in vivo* – for example, starting with non-classical monocytes via deletion of the *Nr4a1* super-enhancer subdomain [70].

Prior to our work, particularly in humans, the dynamics of the distinct subsets of lung macrophages in PH, mainly alveolar and interstitial, had not been defined. While the importance of interstitial macrophages has been described in PH previously [21, 71], the contribution of alveolar macrophages to pathogenesis is unclear. In contrast to the progressive expansion of interstitial macrophages, we found that alveolar macrophages were decreased in both rodent and human instances of PH. To our knowledge, alveolar macrophages have not previously been quantified in depth in human PH, but other groups have conversely reported their increase [72] and activation [73] in chronically hypoxic mice. These discrepancies may be explained by a recent report delineating a spatio-temporal program of at times divergent alveolar and interstitial macrophage activation in hypoxic lungs of mice [21]. It remains unclear whether such complex cellular programming of alveolar macrophages exists in the development of human PH as well. Nonetheless, the functional consequences of the decrease of alveolar macrophages observed in our study are not fully understood. Since alveolar macrophages are known to participate in local immune homeostasis [14, 15] and offer protection from viral infections such as influenza [74], it

Author Manuscript Author Manuscript Author Manuscript Author Manuscript

would be intriguing to determine whether such changes may predispose to the development of certain types of PAH that rely upon infectious (*i.e.*, human immunodeficiency virus infection) or autoimmune (*i.e.*, connective tissue disease) etiologies.

While substantial evidence is mounting regarding the pathogenic importance of interstitial macrophage expansion and inflammation in PH, prior studies have failed to define the exact downstream parameters by which these cells exert their influence on the pulmonary vasculature. Both pulmonary vascular hemodynamics and histopathology are thought to actively contribute to direct disease pathogenesis, and these indices can be simultaneously affected by macrophage disruption [22, 72], particularly at severe, end-stage disease. In contrast, our results demonstrate that, in multiple separate examples of rodent PH, pulmonary vascular remodeling rather than hemodynamic dysfunction is under more robust macrophage-dependent control. Namely, we found that inhibition of Cx_3cr1/Ccr2 signaling and consequent decrease in interstitial macrophage expansion potently reduced pulmonary vascular remodeling and inflammation with a less robust hemodynamic amelioration in two rodent models of PH. Consistent with our findings, previous work has suggested that macrophage depletion via a pharmacologic means in hypoxic mice can improve vascular remodeling without mention of any hemodynamic improvements [2]. Furthermore, more recent evidence suggests other contexts where inflammatory injury may display such dissociation [75]. The molecular etiologies of this dissociation remain unclear, but this observation appears to emphasize the distinct immunologic cues controlling vascular hyperproliferation rather than vasomotor tone. Given this observation coupled with the distinct spatio-temporal cues that govern macrophage expansion in PH [21], it may also be possible that dissociation is more prominent when comparing early versus late stage PH or comparing specific anatomic compartments of the pulmonary vascular tree. Future delineation of this hypothesis will necessitate an ability to follow simultaneous tissue remodeling with hemodynamics over the course of disease – technology that is not currently available for human study but potentially could be envisioned in rodents when coupling molecular imaging with hemodynamic telemetry. This dissociation also has fundamental implications regarding the immunologic nature of vascular lesions in PH. For example, pulmonary vascular remodeling in the absence of increased pulmonary arterial pressures was reversible when induced by inhalation of fungal spores of *Stachybotrys chartarum* [76]. Such reversibility, if applicable to macrophage-dependent vascular alterations reported here, gives credence to the potential efficacy of anti-inflammatory agents for this disease. On the other hand, these data suggest that any anti-inflammatory agents tested in humans should be combined with existing vasodilators or other drug with complementary vasomotor efficacy in order to attain truly durable histologic and hemodynamic improvement.

Our findings also serve as a platform for future translational development in both myeloid-based diagnostics and therapeutics. Diagnostic identification of inflammatory monocytes, especially non-classical monocytes, could aid in prognostic evaluation of PH patients and could serve as a method to identify patients appropriate for emerging immunologic therapy. Whether these cells could be quantified as a measure of timing or severity of disease will depend on future studies defining a timeframe of activation and expansion of pro-inflammatory monocytes and their recruitment to the lungs. Consequent therapeutic targeting of these cells or molecules, such as Cx_3Cl1, that control their expansion could

Author Manuscript Author Manuscript Author Manuscript Author Manuscript

decrease lung inflammation and pathogenic tissue remodeling in PH patients. More sophisticated drug development would predicate on better understanding of the monocyte to lung perivascular macrophage transition, as targeting the precursor monocyte subset before infiltration may be a more effective strategy for entirely preventing tissue inflammation. Moreover, because hemodynamics alone may not fully reflect the potency of a macrophage-depleting agent, our data support the notion of utilizing an independent index of disease progression to evaluate efficacy for any anti-inflammatory agent in future clinical trial design.

Our study reports that chemokine receptors, such as CX_3CR1 and CCR2, are important in the recruitment of monocytes in the setting of pulmonary hypertension. Other groups also highlighted the relevance of these two chemokines in the context of pulmonary hypertension. In *ccl2*-deficient hypoxic mice [72], Amsellem and colleagues showed that the lung vasculature remodeling as well as hemodynamics was comparable to wild type hypoxic mice, which is in contrast to our observation of improved pulmonary remodeling in hypoxic *ccr2*-deficient mice. This discrepancy may be explained by the known compensatory mechanisms of other CCR2 ligands such as CCL7. Additionally, this group did not find a decrease in the number of monocytes in *cx3cr1*-deficient mice [72], despite well-established literature reporting the crucial role of CX_3CR1 in monocyte recruitment and survival [77, 78]. Interestingly, Yu and colleagues found increased pulmonary artery muscularization in $ccr2^{-/-}$ mice due to dysregulation of Notch signaling [79]. Yet, in line with our findings, another group reported that *ccr2*-deficiency alleviates angiotensin II-induced vascular remodeling by suppressing blood monocytosis [80]. The phenotypic variations of *ccl2/ccr2* and *cx3cl1/cx3cr1* axis depicted by these different publications highlight the complex biology of the chemokines and their under-explored roles in pulmonary hypertension. To define accurately the biological mechanisms by which these chemokines act in PH, the study of mice with myeloid-specific deficiency of *ccr2* and *cx_3cr1* will be important. Further ablation of these chemokine receptors in myeloid cells after PH has been established may also reveal a context-specific pathobiology controlled by these molecules.

In summary, we have found that monocyte expansion is one of the key immunologic features of PH. The recruitment of inflammatory monocytes into the lungs of PH patients and their subsequent differentiation into interstitial macrophages increases the inflammatory component of PH, primarily affecting pulmonary vascular remodeling. Based on these results, diagnostic identification coupled with therapeutic targeting of this monocyte to macrophage transition may hold great promise in this disease.

Supplementary Material

Refer to Web version on PubMed Central for supplementary material.

Acknowledgments

We would like to acknowledge the NIH supported microscopy resources in the Center for Biologic Imaging. Specifically, the confocal microscope supported by grant number 1S10OD019973-01. Figure 7D was adapted from the Servier Medical Art (www.smart.servier.com)

Author Manuscript Author Manuscript Author Manuscript Author Manuscript

This work was supported by National Institute of Health grant HL121076-03 (to PD) and HL096834, HL124021, and HL138437 (to SYC).

References

1. Sawada H, et al. Reduced BMPR2 expression induces GM-CSF translation and macrophage recruitment in humans and mice to exacerbate pulmonary hypertension. J Exp Med. 2014; 211(2): 263–80. [PubMed: 24446489]
2. Frid MG, et al. Hypoxia-induced pulmonary vascular remodeling requires recruitment of circulating mesenchymal precursors of a monocyte/macrophage lineage. Am J Pathol. 2006; 168(2):659–69. [PubMed: 16436679]
3. Hwangbo C, et al. Modulation of Endothelial BMPR2 Activity by VEGFR3 in Pulmonary Arterial Hypertension. Circulation. 2017
4. Mathew R, et al. Hematological disorders and pulmonary hypertension. World J Cardiol. 2016; 8(12):703–718. [PubMed: 28070238]
5. Mouraret N, et al. Activation of lung p53 by Nutlin-3a prevents and reverses experimental pulmonary hypertension. Circulation. 2013; 127(16):1664–76. [PubMed: 23513067]
6. Vergadi E, et al. Early macrophage recruitment and alternative activation are critical for the later development of hypoxia-induced pulmonary hypertension. Circulation. 2011; 123(18):1986–95. [PubMed: 21518986]
7. Tian W, et al. Blocking macrophage leukotriene b4 prevents endothelial injury and reverses pulmonary hypertension. Sci Transl Med. 2013; 5(200):200ra117.
8. Perrin S, et al. New pharmacotherapy options for pulmonary arterial hypertension. Expert Opin Pharmacother. 2015; 16(14):2113–31. [PubMed: 26290279]
9. Taichman DB, et al. Pharmacologic therapy for pulmonary arterial hypertension in adults: CHEST guideline and expert panel report. Chest. 2014; 146(2):449–75. [PubMed: 24937180]
10. El Kasmi KC, et al. Adventitial fibroblasts induce a distinct proinflammatory/profibrotic macrophage phenotype in pulmonary hypertension. J Immunol. 2014; 193(2):597–609. [PubMed: 24928992]
11. Tuder RM, et al. Exuberant endothelial cell growth and elements of inflammation are present in plexiform lesions of pulmonary hypertension. Am J Pathol. 1994; 144(2):275–85. [PubMed: 7508683]
12. Dorfmuller P, et al. Inflammation in pulmonary arterial hypertension. Eur Respir J. 2003; 22(2): 358–63. [PubMed: 12952274]
13. Savai R, et al. Immune and inflammatory cell involvement in the pathology of idiopathic pulmonary arterial hypertension. Am J Respir Crit Care Med. 2012; 186(9):897–908. [PubMed: 22955318]
14. Trapnell BC, Whitsett JA. Gm-CSF regulates pulmonary surfactant homeostasis and alveolar macrophage-mediated innate host defense. Annu Rev Physiol. 2002; 64:775–802. [PubMed: 11826288]
15. Dranoff G, et al. Involvement of granulocyte-macrophage colony-stimulating factor in pulmonary homeostasis. Science. 1994; 264:713. [PubMed: 8171324]
16. Franke-Ullmann G, et al. Characterization of murine lung interstitial macrophages in comparison with alveolar macrophages in vitro. The Journal of Immunology. 1996; 157(7):3097–3104. [PubMed: 8816420]
17. Bedoret D, et al. Lung interstitial macrophages alter dendritic cell functions to prevent airway allergy in mice. The Journal of Clinical Investigation. 2009; 119(12):3723–3738. [PubMed: 19907079]
18. Laskin DL, Weinberger B, Laskin JD. Functional heterogeneity in liver and lung macrophages. J Leukoc Biol. 2001; 70(2):163–70. [PubMed: 11493607]
19. Bryant AJ, et al. Expression of mutant bone morphogenetic protein receptor II worsens pulmonary hypertension secondary to pulmonary fibrosis. Pulm Circ. 2015; 5(4):681–90. [PubMed: 26697175]

Author Manuscript Author Manuscript Author Manuscript Author Manuscript

20. Yan L, et al. Bone Marrow-derived Cells Contribute to the Pathogenesis of Pulmonary Arterial Hypertension. Am J Respir Crit Care Med. 2016; 193(8):898–909. [PubMed: 26651104]
21. Pugliese SC, et al. A Time- and Compartment-Specific Activation of Lung Macrophages in Hypoxic Pulmonary Hypertension. J Immunol. 2017; 198(12):4802–4812. [PubMed: 28500078]
22. Kumar R, et al. TGF-beta activation by bone marrow-derived thrombospondin-1 causes Schistosoma- and hypoxia-induced pulmonary hypertension. Nat Commun. 2017; 8:15494. [PubMed: 28555642]
23. Misharin AV, et al. Flow cytometric analysis of macrophages and dendritic cell subsets in the mouse lung. Am J Respir Cell Mol Biol. 2013; 49(4):503–10. [PubMed: 23672262]
24. Yona S, et al. Fate mapping reveals origins and dynamics of monocytes and tissue macrophages under homeostasis. Immunity. 2013; 38(1):79–91. [PubMed: 23273845]
25. Orkin SH, Zon LI. Hematopoiesis: an evolving paradigm for stem cell biology. Cell. 2008; 132(4): 631–44. [PubMed: 18295580]
26. Davies LC, et al. Tissue-resident macrophages. Nat Immunol. 2013; 14(10):986–95. [PubMed: 24048120]
27. Geissmann F, Jung S, Littman DR. Blood monocytes consist of two principal subsets with distinct migratory properties. Immunity. 2003; 19(1):71–82. [PubMed: 12871640]
28. Auffray C, et al. Monitoring of blood vessels and tissues by a population of monocytes with patrolling behavior. Science. 2007; 317(5838):666–70. [PubMed: 17673663]
29. Ingersoll MA, et al. Comparison of gene expression profiles between human and mouse monocyte subsets. Blood. 2010; 115(3):e10–9. [PubMed: 19965649]
30. Mukherjee R, et al. Non-Classical monocytes display inflammatory features: Validation in Sepsis and Systemic Lupus Erythematous. Sci Rep. 2015; 5:13886. [PubMed: 26358827]
31. Zimmermann HW, et al. Functional contribution of elevated circulating and hepatic non-classical CD14CD16 monocytes to inflammation and human liver fibrosis. PLoS One. 2010; 5(6):e11049. [PubMed: 20548789]
32. Ramirez R, et al. Microinflammation in hemodialysis is related to a preactivated subset of monocytes. Hemodial Int. 2006; 10(Suppl 1):S24–7.
33. Jacquelin S, et al. CX3CR1 reduces Ly6Chigh-monocyte motility within and release from the bone marrow after chemotherapy in mice. Blood. 2013; 122(5):674–83. [PubMed: 23775714]
34. Landsman L, et al. CX3CR1 is required for monocyte homeostasis and atherogenesis by promoting cell survival. Blood. 2009; 113(4):963–72. [PubMed: 18971423]
35. Serbina NV, Pamer EG. Monocyte emigration from bone marrow during bacterial infection requires signals mediated by chemokine receptor CCR2. Nat Immunol. 2006; 7(3):311–7. [PubMed: 16462739]
36. Kurihara T, et al. Defects in macrophage recruitment and host defense in mice lacking the CCR2 chemokine receptor. J Exp Med. 1997; 186(10):1757–62. [PubMed: 9362535]
37. Guilliams M, et al. Alveolar macrophages develop from fetal monocytes that differentiate into long-lived cells in the first week of life via GM-CSF. J Exp Med. 2013; 210(10):1977–92. [PubMed: 24043763]
38. Davies LC, et al. Distinct bone marrow-derived and tissue-resident macrophage lineages proliferate at key stages during inflammation. Nat Commun. 2013; 4:1886. [PubMed: 23695680]
39. Gomez-Arroyo JG, et al. The monocrotaline model of pulmonary hypertension in perspective. Am J Physiol Lung Cell Mol Physiol. 2012; 302(4):L363–9. [PubMed: 21964406]
40. Auffray C, Sieweke MH, Geissmann F. Blood monocytes: development, heterogeneity, and relationship with dendritic cells. Annu Rev Immunol. 2009; 27:669–92. [PubMed: 19132917]
41. Shi C, Pamer EG. Monocyte recruitment during infection and inflammation. Nat Rev Immunol. 2011; 11(11):762–74. [PubMed: 21984070]
42. Dutta P, et al. Myocardial infarction accelerates atherosclerosis. Nature. 2012; 487(7407):325–9. [PubMed: 22763456]
43. Tsou CL, et al. Critical roles for CCR2 and MCP-3 in monocyte mobilization from bone marrow and recruitment to inflammatory sites. J Clin Invest. 2007; 117(4):902–9. [PubMed: 17364026]

Author Manuscript Author Manuscript Author Manuscript Author Manuscript

44. Franke-Ullmann G, et al. Characterization of murine lung interstitial macrophages in comparison with alveolar macrophages in vitro. J Immunol. 1996; 157(7):3097–104. [PubMed: 8816420]
45. Tan SY, Krasnow MA. Developmental origin of lung macrophage diversity. Development. 2016; 143(8):1318–27. [PubMed: 26952982]
46. Serbina NV, et al. Monocyte-mediated defense against microbial pathogens. Annu Rev Immunol. 2008; 26:421–52. [PubMed: 18303997]
47. Carlin LM, et al. Nr4a1-dependent Ly6C(low) monocytes monitor endothelial cells and orchestrate their disposal. Cell. 2013; 153(2):362–75. [PubMed: 23582326]
48. Dutta P, Nahrendorf M. Monocytes in myocardial infarction. Arterioscler Thromb Vasc Biol. 2015; 35(5):1066–70. [PubMed: 25792449]
49. Gu X, et al. Fractalkine neutralization improves cardiac function after myocardial infarction. Exp Physiol. 2015; 100(7):805–17. [PubMed: 25943588]
50. Bronte V. The spleen in local and systemic regulation of immunity. 2013; 39(5):806–18.
51. Lanzola E, et al. Bone marrow-derived vascular modulatory cells in pulmonary arterial hypertension. Pulm Circ. 2013; 3(4):781–91. [PubMed: 25006394]
52. Spees JL, et al. Bone marrow progenitor cells contribute to repair and remodeling of the lung and heart in a rat model of progressive pulmonary hypertension. Faseb j. 2008; 22(4):1226–36. [PubMed: 18032636]
53. Chan SY, Loscalzo J. Pathogenic mechanisms of pulmonary arterial hypertension. J Mol Cell Cardiol. 2008; 44(1):14–30. [PubMed: 17950310]
54. Rorholt M, et al. Risk of cardiovascular events and pulmonary hypertension following splenectomy - a Danish population-based cohort study from 1996–2012. Haematologica. 2017; 102(8):1333–1341. [PubMed: 28572164]
55. Segraves JM, et al. The Relationship Between Portopulmonary Hypertension and Splenectomy: Mayo Clinic Experience and Literature Review. Hepatol Res. 2017
56. Palkar AV, et al. Post splenectomy related pulmonary hypertension. World J Respirol. 2015; 5(2): 69–77. [PubMed: 26949600]
57. Ferraro F, et al. Diabetes impairs hematopoietic stem cell mobilization by altering niche function. Sci Transl Med. 2011; 3(104):104ra101.
58. Perin PC, Maule S, Quadri R. Sympathetic nervous system, diabetes, and hypertension. Clin Exp Hypertens. 2001; 23(1–2):45–55. [PubMed: 11270588]
59. Schuettpelz LG, Link DC. Regulation of Hematopoietic Stem Cell Activity by Inflammation. Front Immunol. 2013:4. [PubMed: 23386848]
60. Woollard KJ, Geissmann F. Monocytes in atherosclerosis: subsets and functions. Nat Rev Cardiol. 2010; 7(2):77–86. [PubMed: 20065951]
61. Weber C, Zernecke A, Libby P. The multifaceted contributions of leukocyte subsets to atherosclerosis: lessons from mouse models. Nat Rev Immunol. 2008; 8(10):802–15. [PubMed: 18825131]
62. Tacke F, et al. Monocyte subsets differentially employ CCR2, CCR5, and CX3CR1 to accumulate within atherosclerotic plaques. J Clin Invest. 2007; 117(1):185–94. [PubMed: 17200718]
63. Saederup N, et al. Fractalkine deficiency markedly reduces macrophage accumulation and atherosclerotic lesion formation in CCR2−/− mice: evidence for independent chemokine functions in atherogenesis. Circulation. 2008; 117(13):1642–8. [PubMed: 18165355]
64. Lesnik P, Haskell CA, Charo IF. Decreased atherosclerosis in CX3CR1−/− mice reveals a role for fractalkine in atherogenesis. J Clin Invest. 2003; 111(3):333–40. [PubMed: 12569158]
65. Swirski FK, et al. Ly-6Chi monocytes dominate hypercholesterolemia-associated monocytosis and give rise to macrophages in atheromata. J Clin Invest. 2007; 117(1):195–205. [PubMed: 17200719]
66. Swirski FK, Weissleder R, Pittet MJ. Heterogeneous in vivo behavior of monocyte subsets in atherosclerosis. Arterioscler Thromb Vasc Biol. 2009; 29(10):1424–32. [PubMed: 19372462]
67. Tsujioka H, et al. Impact of heterogeneity of human peripheral blood monocyte subsets on myocardial salvage in patients with primary acute myocardial infarction. J Am Coll Cardiol. 2009; 54(2):130–8. [PubMed: 19573729]

Author Manuscript Author Manuscript Author Manuscript Author Manuscript

68. Nahrendorf M, et al. The healing myocardium sequentially mobilizes two monocyte subsets with divergent and complementary functions. J Exp Med. 2007; 204(12):3037–47. [PubMed: 18025128]
69. Nahrendorf M, Pittet MJ, Swirski FK. Monocytes: protagonists of infarct inflammation and repair after myocardial infarction. Circulation. 2010; 121(22):2437–45. [PubMed: 20530020]
70. Thomas GD, et al. Deleting an Nr4a1 Super-Enhancer Subdomain Ablates Ly6Clow Monocytes while Preserving Macrophage Gene Function. Immunity. 2016; 45(5):975–987. [PubMed: 27814941]
71. Jankov RP, et al. Gadolinium chloride inhibits pulmonary macrophage influx and prevents O(2)-induced pulmonary hypertension in the neonatal rat. Pediatr Res. 2001; 50(2):172–83. [PubMed: 11477200]
72. Amsellem V, et al. Roles for the CX3CL1/CX3CR1 and CCL2/CCR2 Chemokine Systems in Hypoxic Pulmonary Hypertension. Am J Respir Cell Mol Biol. 2017
73. Zaloudikova M, et al. Depletion of alveolar macrophages attenuates hypoxic pulmonary hypertension but not hypoxia-induced increase in serum concentration of MCP-1. Physiol Res. 2016; 65(5):763–768. [PubMed: 27429111]
74. Schneider C, et al. Alveolar macrophages are essential for protection from respiratory failure and associated morbidity following influenza virus infection. PLoS Pathog. 2014; 10(4):e1004053. [PubMed: 24699679]
75. Chen PI, et al. Amphetamines promote mitochondrial dysfunction and DNA damage in pulmonary hypertension. JCI Insight. 2017; 2(2):e90427. [PubMed: 28138562]
76. Nagayoshi M, et al. Inhalation of Stachybotrys chartarum evokes pulmonary arterial remodeling in mice, attenuated by Rho-kinase inhibitor. Mycopathologia. 2011; 172(1):5–15. [PubMed: 21505873]
77. Combadiere C, et al. Combined inhibition of CCL2, CX3CR1, and CCR5 abrogates Ly6C(hi) and Ly6C(lo) monocytosis and almost abolishes atherosclerosis in hypercholesterolemic mice. Circulation. 2008; 117(13):1649–57. [PubMed: 18347211]
78. Cochain C, et al. Regulation of monocyte subset systemic levels by distinct chemokine receptors controls post-ischaemic neovascularization. Cardiovasc Res. 2010; 88(1):186–95. [PubMed: 20501509]
79. Yu YR, et al. CCR2 deficiency, dysregulation of Notch signaling, and spontaneous pulmonary arterial hypertension. Am J Respir Cell Mol Biol. 2013; 48(5):647–54. [PubMed: 23492191]
80. Ishibashi M, et al. Critical role of monocyte chemoattractant protein-1 receptor CCR2 on monocytes in hypertension-induced vascular inflammation and remodeling. Circ Res. 2004; 94(9): 1203–10. [PubMed: 15059935]

Author Manuscript Author Manuscript Author Manuscript Author Manuscript

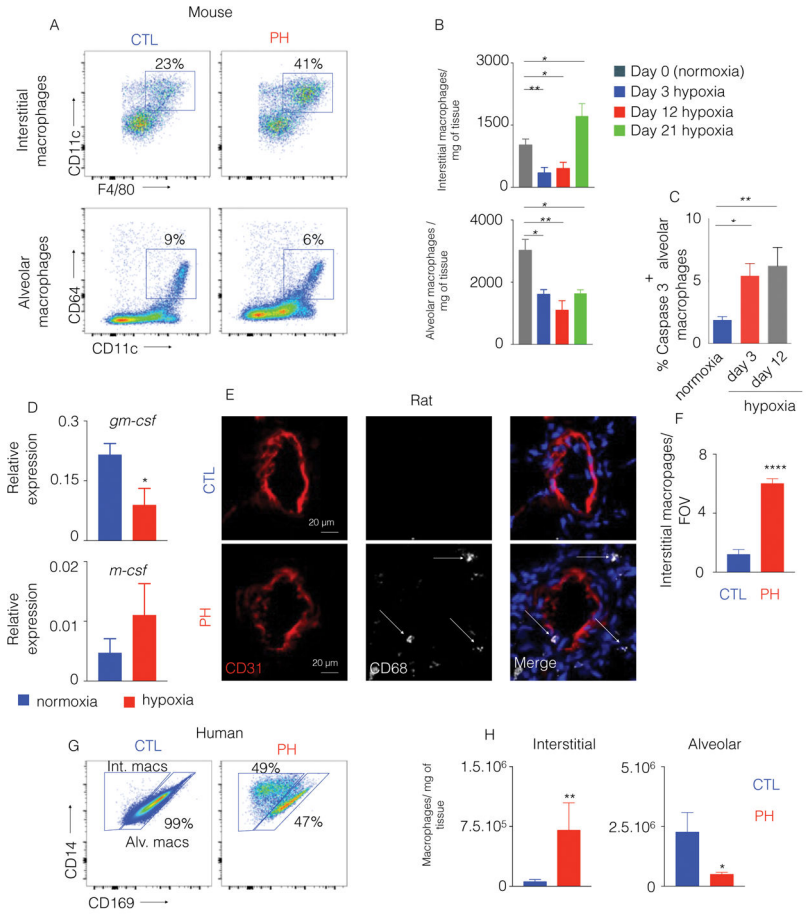

Figure 1. The number of lung interstitial macrophages is increased in hypoxic mice, monocrotaline-injected rats and patients

C57BL/6 mice were placed in normoxia or hypoxia (n=5 per group) for three weeks to induce PH. **A**) Representative flow cytometric plots for murine alveolar and interstitial macrophages in the lungs are shown, with **B)** quantification of these cells at different time points after hypoxia exposure. **C)** Percentage of caspase 3 positive alveolar macrophages in normoxic and hypoxic mice was determined by flow cytometry. **D)** Quantification of *gm-csf* and *m-csf* in the lungs of hypoxic mice compared to normoxic controls. **E**) Confocal imaging of lung sections were stained for CD31 and CD68 in monocrotaline-injected rats, and **F)** quantification of $CD68^+$ interstitial perivascular macrophages in monocrotaline-injected rats was pursued. n=5 control rats and 5 MCT rats. **G)** Flow cytometric plots display the proportions of human alveolar vs. interstitial macrophages in control (CTL) and PH lung samples. **H)** Quantitation of human alveolar and interstitial macrophages is shown. n=5 healthy donors and 6 PAH patients. Mean ± s.e.m. * $P < 0.05$, ** $P < 0.01$, **** $P < 0.001$.

Author Manuscript Author Manuscript Author Manuscript Author Manuscript

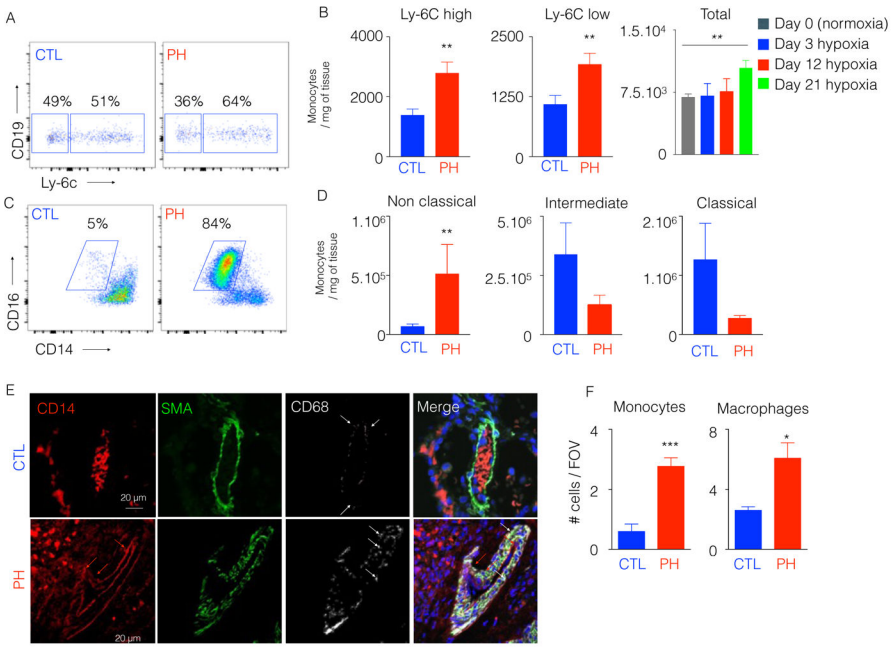

Figure 2. The number of inflammatory lung monocytes is elevated in hypoxic mice and PAH patients

C57BL/6 mice were placed in a 10% O_2 hypoxic chamber (n=4 normoxic controls and 6 hypoxic mice) for three weeks to induce PH. **A**) Flow cytometric plots showing the proportion of Ly-6C^{high} and Ly-6C^{low} monocytes in hypoxic and normoxic mouse lung samples. **B)** Quantitation of Ly-6C^{high} and Ly-6C^{low} monocytes at 21 days, and total monocytes at various timepoints after hypoxia initiation **C**) PAH patient lung samples (n=6) or control lung samples (n=5) were collected. Flow cytometric plots showing the proportion of lung non-classical monocytes in control (CTL) and PAH patients. **D)** Quantitation of classical, intermediate and non-classical monocytes in CTL and PAH lung samples. **E)** Confocal imaging of patient lung sections stained for CD68, SMA and CD14. **F**) Quantification of monocytes and macrophages in CTL and PAH lung samples. Mean ± s.e.m. ** P < 0.01.

Author Manuscript Author Manuscript Author Manuscript Author Manuscript

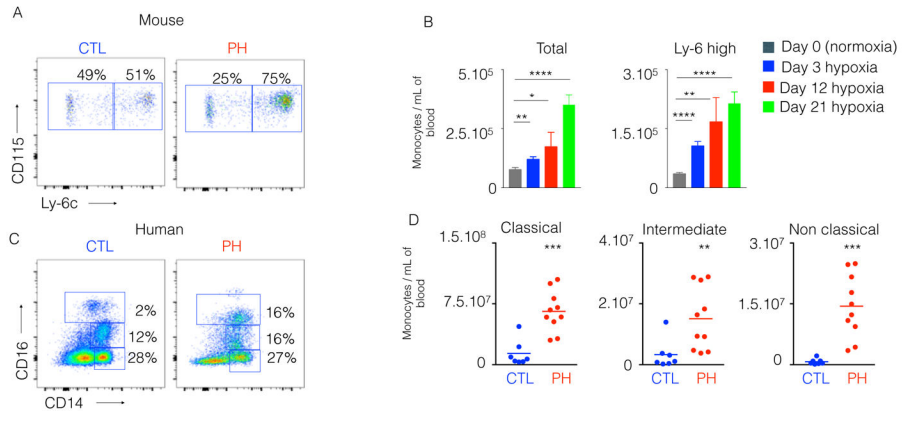

Source	% of cell population	CTL	PAH patient
Lung	Alveolar macrophages	72	24
	Interstitial macrophages	25	72
	Classical monocytes	85	16
	Intermediate monocytes	1	2
	Non classical monocytes	4	12
Blood	Classical monocytes	25	51
	Intermediate monocytes	14	22
	Non classical monocytes	2	16

Figure 3. Circulatory inflammatory monocytes were increased in hypoxic mice and PAH patients

C57BL/6 mice were placed in a 10% O_2 hypoxic chamber (n=4 normoxic and 6 hypoxic mice) for three weeks to induce PH. **A**) The flow cytometric plots show the proportion of circulatory Ly-6C^{high} and Ly-6C^{low} monocytes in hypoxic and normoxic mice and **B)** Quantification of total monocytes and Ly-6C^{high} monocytes at various timepoints after hypoxic exposure. **C)** Blood from PAH patients (n=9) and healthy donors (n=7) was collected. Flow cytometric plots show the proportion of blood inflammatory monocytes in control (CTL) and PH patients. **D)** Quantification of classical, intermediate and non-classical monocytes is shown in both CTL and PAH blood samples. **E)** Blood and lung samples were collected from a PH patient. The frequency of lung macrophage and circulatory monocyte subsets of a healthy control and the PAH patient is shown in the table. **F)** Confocal images of lung sections of the PH patient are displayed. The sections were stained for CD68, SMA and CD14. Mean ± s.e.m., ** P < 0.01, *** P<0.001 **** P < 0.0001.

Author Manuscript Author Manuscript Author Manuscript Author Manuscript

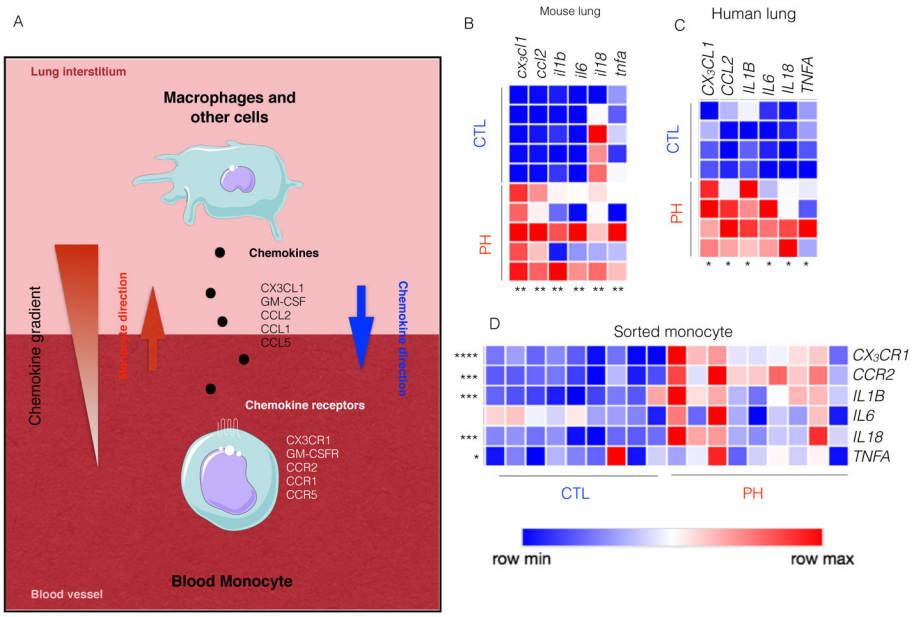

Figure 4. Hypoxic mice and patients with PH had increased levels of cytokines, chemokines and chemokine receptors

C57BL/6 mice were placed in a 10% O_2 hypoxic chamber (n=5 per group) for three weeks to induce PH. **A)** Schematic diagram shows that lung chemokines trigger the active recruitment of blood monocytes to the lungs. Adapted from the Medical Servier of Art. **B)** Quantitation of *cx3cl1, ccl2, il1b, il6, il18* and *tnfa* mRNA expression in the lungs of hypoxic and normoxic mice. Blood and lung samples from PAH patients (n=9) and healthy donors (n=7) were collected. **C)** Quantitation of *CX3CL1, CCL2, IL1B, IL6, IL18,* and *TNFA* expression in the lungs of PH patients and healthy controls. **D)** Quantitation of chemokine receptors and pro-inflammatory cytokines mRNA expression such as *CX3CL1, CCL2, IL1B, IL6, IL18,* and *TNFA* by monocytes sorted from the blood of PH patients and healthy controls. Mean ± s.e.m., * P < 0.05 ** P < 0.01, *** P< 0.001 **** P < 0.0001.

Author Manuscript Author Manuscript Author Manuscript Author Manuscript

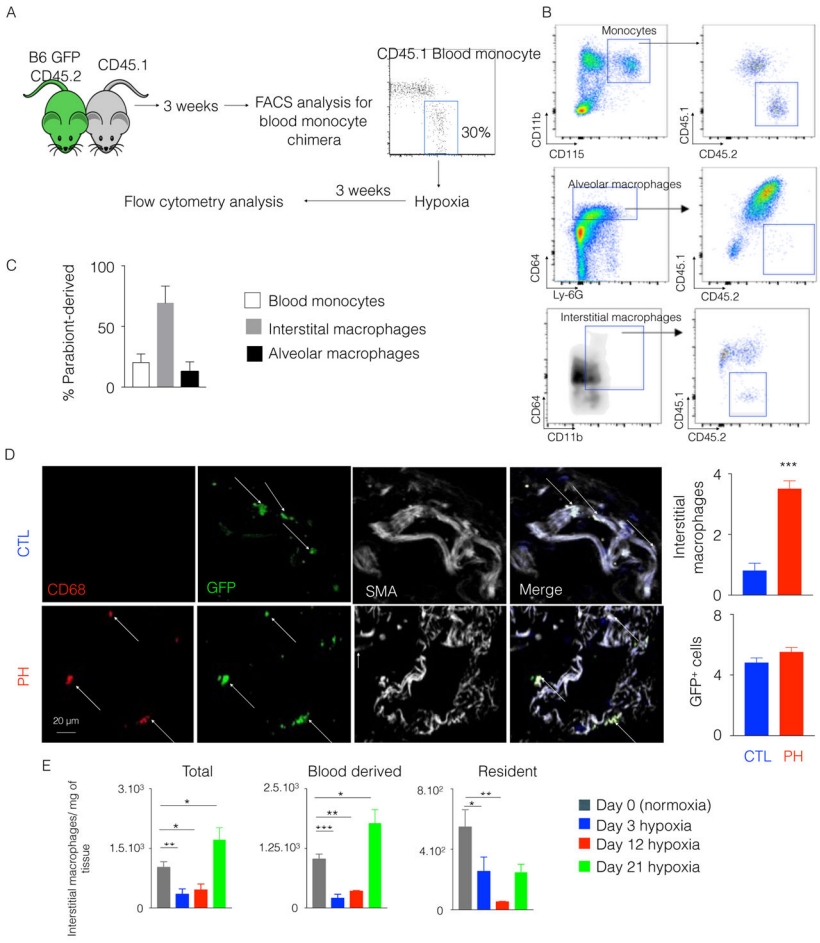

Figure 5. Parabiosis between hypoxic mice demonstrated the monocytic origin of interstitial macrophages in the lungs

A) CD45.1 C57BL/6 mouse and CD45.2 GFP C57BL/6 mouse were surgically joined. Three weeks after the parabiosis, they were placed in a hypoxic chamber for 3 weeks. **B)** Flow cytometric plots show the chimera levels in blood monocytes and lung macrophages of hypoxic mice. **C)** The histogram shows the percentage of $CD45.2^+$ parabiont-derived cells in blood monocytes, interstitial macrophages and alveolar macrophages in CD45.1 hypoxic mice. **D)** Confocal imaging of lung sections of the $CD45.1^+$ parabionts shows GFP^+ interstitial perivascular macrophages. **E)** Flow cytometric enumeration of total, monocyte-derived and resident interstitial macrophages in the lungs of hypoxic mice and normoxic controls. n=4 mice per group. Mean ± s.e.m, * P < 0.05 ** P < 0.01, *** P< 0.001 ****.

Author Manuscript Author Manuscript Author Manuscript Author Manuscript

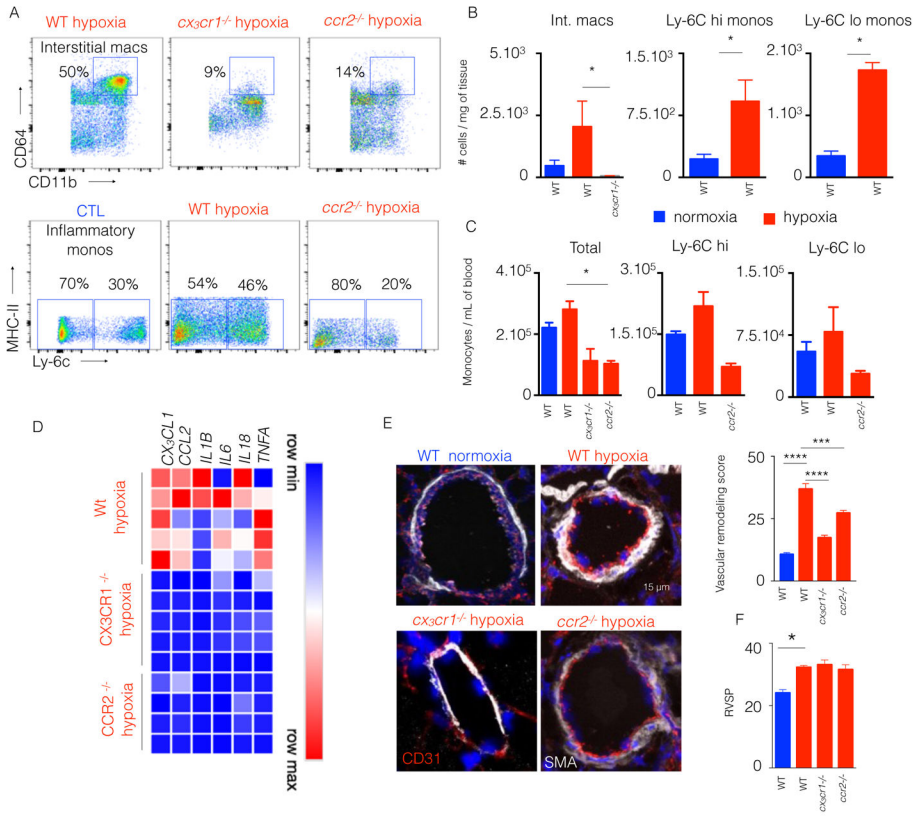

Figure 6. CCR2 and CX$_3$CR1 deficient mice had an attenuated lung remodeling

ccr2$^{-/-}$ and *cx$_3$cr1*$^{-/-}$ mice were put in hypoxic chambers for 3 weeks. n= 5 normoxic wild type (WT) mice, 5 hypoxic WT mice, 5 hypoxic *cx$_3$cr1*$^{-/-}$ mice and 5 *ccr2*$^{-/-}$ hypoxic mice. **A)** Flow plots showing the proportions of interstitial macrophages and monocytes in WT, *ccr2*$^{-/-}$ and *cx3cr1*$^{-/-}$ mice. **B)** The histograms show the number of total monocytes, Ly-6C^{high} monocytes and Ly-6C^{low} monocytes in the lungs. **C)** Histograms showing the number of interstitial macrophages, Ly-6C^{high} monocytes and Ly-6C^{low} monocytes in the blood of WT, *cx3cr1*$^{-/-}$ and *ccr2*$^{-/-}$ mice. **D)** Quantitation of mRNA levels of chemokines and pro-inflammatory cytokines in the lungs. **E)** Confocal images of lung sections stained for CD31 and SMA. **F)** Histograms showing right ventricular systolic pressure (RVSP). Mean ± s.e.m., * P < 0.05, *** P< 0.001, **** P < 0.0001.

Author Manuscript Author Manuscript Author Manuscript Author Manuscript

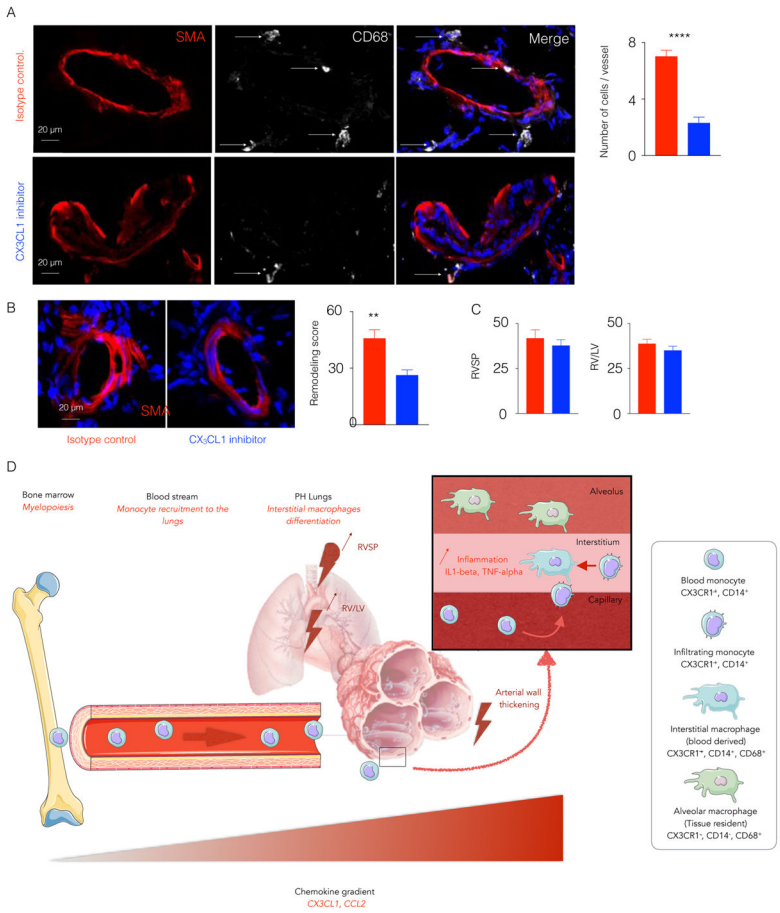

Figure 7. Cx_3cl1 inhibitor limited the recruitment of monocytes in monocrotaline-injected rats

Adult male Sprague-Dawley rats were injected once with monocrotaline to induce PH. The rats were injected with either Cx_3cl1 inhibitor or isotype antibody for 3 weeks. **A)** Confocal imaging of lung sections stained for CD68 and SMA. The histogram quantifies lung perivascular macrophages. **B)** The confocal images of lung sections stained for SMA show the lung vasculature remodeling. Remodeling score was quantified. **C)** The histograms show right ventricular systolic pressure and RV/LV ratio in isotype control and Cx_3cl1 inhibitor-injected rats. n=5 per group, Mean ± s.e.m., ** P< 0.01, **** P < 0.001. **D)** The schematic diagram depicts monocyte recruitment to the lungs and expansion of interstitial macrophages in PH. CX_3CR1^+ $CCR2^+$ monocytes egress from the bone marrow into the blood stream. The production of chemokines, such as CX_3CL1 and CCL2, in the lungs and increased expression of the receptors of these chemokines on circulatory monocytes mediate their recruitment into the lungs in the context of PH. These newly recruited monocytes differentiate into interstitial perivascular macrophages. Adapted from the Medical Servier of Art.